Microsc. Microanal. Microstruct. **6** (1995) 237–248 APRIL **1995**, PAGE 237

Classification
Physics Abstracts
61.16Di — 61.50Jr — 68.55Jk

HRTEM Studies of the Epitaxial Growth of Pd Particles (1 – 6 nm) on ZnO Micro- Prisms

Suzanne Giorgio, Claude R. Henry and Claude Chapon

CRMC2-CNRS, Campus de Luminy, Case 913, 13288 Marseille Cedex 9, France

(Received January 30; accepted March 21, 1995)

Abstract. — Pd particles (1 – 6 nm) were grown under UHV conditions from a Knudsen cell, on small ZnO prisms *in situ* prepared in a controlled atmosphere. 3-D Pd particles epitaxially oriented on the ZnO faces were observed by HRTEM, both in top view and in profile view on the lateral (10.0) faces of the ZnO prisms. The epitaxial relations were determined: $(211)_{Pd} \parallel (10.0)_{ZnO}$ and $[011]_{Pd} \parallel [001]_{ZnO}$. From the HRTEM observations of the single ZnO prisms and the tetrapods twins, the precise structure of the central ZnO nucleus was also evidenced.

1. Introduction

Small supported particles used as model catalysts (Pd, Pt, Rh, Cu, Ni), are often prepared by condensation of metal in UHV conditions on oxides single crystals, such as MgO [1], TiO_2 [2], Al_2O_3 [3]. Among the different techniques of electron microscopy, HRTEM profile imaging is the best method for studying the morphology of the particles and the structure of their interface with the substrate [4, 5]. In the case of oxides, micro- crystals with regular shapes are convenient for imaging both top and profile views of the particles [5-7].

Pd or Cu particles prepared on ZnO have industrial applications as catalysts in the methanol synthesis [8-13].

ZnO smokes have been widely studied for their interesting growth mechanism and twinnings [14-17]. They were produced by oxidation of the Zn metal heated at high temperature in a boat under Oxygen pressure. Then smokes samples were collected at different distances from the Zn source [14]. Near the boat, most of the smokes were found as octahedra of cubic blende structure, limited by 4 (111) faces of oxygen and 4 (111) faces of Zn. Further away from the boat, smokes are micro- prisms of hexagonal wurtzite structure elongated along the *c* axis, most of them are twinned as tetrapods with four legs connected to a common octahedral nucleus. According to the different authors, the structure of this nucleus is of blende type [14, 15] or wurtzite type [16, 17]. Our HRTEM images give further arguments to determine this structure.

In this paper, Pd particles are grown by condensation in UHV conditions on clean lateral faces (10.0) of ZnO micro- prisms *in situ* prepared. The shape and epitaxial orientations of the Pd particles are determined by HRTEM images of the surface and the edges of ZnO.

2. Sample Preparation

ZnO prisms were produced in a UHV chamber by burning a Zn filament in a mixture of pure O_2 (70%) and N_2 (30%) gases and collected (*in situ*) on a microscope grid covered with a carbon film. This technique was already described in the case of MgO smokes [5]. The grid fixed on a rotating furnace was heated to 450 °C while the chamber was evacuated to the pressure 7×10^{-10} Torr. At this pressure and temperature, the grid was brought in front of a Knudsen cell for the Pd condensation. The metal flux was calibrated to 1×10^{13} atoms cm^{-2} s^{-1}. The pressure during the evaporation increased up to 5×10^{-9} Torr. The samples were covered with a carbon layer to avoid contamination and to allow the observations in electron microscopy without charging effects of the ZnO.

3. HRTEM Observations

The samples were observed either with a Jeol 4000EX microscope operating at 400 KV, or with a Philips CM30 microscope operating at 300 KV and equiped with super twins polar pieces. Figure 1a is an overview of the Pd particles on a ZnO tetrapod support. From different samples, the particle size varies between 1 and 6 nm. Figure 1b indicates the indices of the different faces limiting the ZnO prisms.

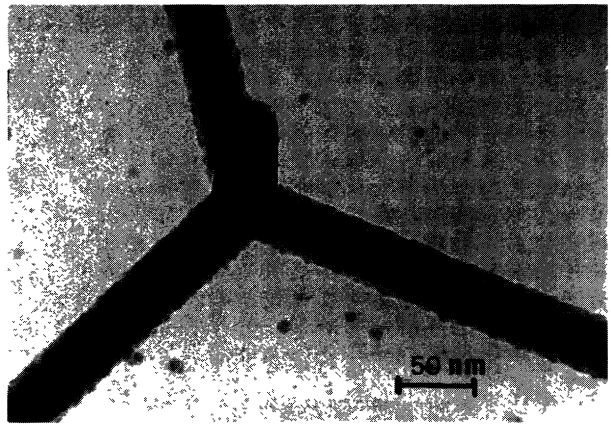

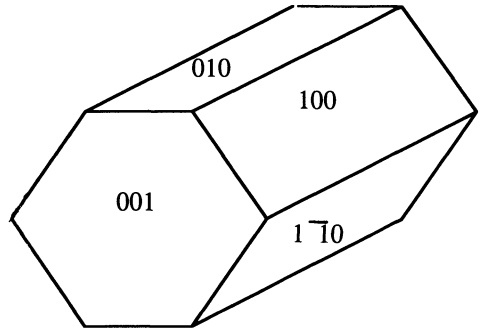

Fig. 1. — a) Tetrapod like ZnO crystals with Pd particles on the surfaces. b) Indexing of the facets limiting the ZnO prisms. Lateral faces are (10.0), (01.0), and (1 $\bar{1}$.0) are neutral while basal faces (00.1) are polar.

Figure 2 shows an high resolution image of two ZnO legs connected to the same nucleus, both normal to the electron beam and observed along a common [210] direction. In this orientation, the electron beam is perpendicular to a pair of lateral (10.0) faces in both prisms of wurtzite structure. The power spectrum (PS) of the image of a prism, far from the nucleus, is given in the inset, in the vertical leg. It contains the [002]* and [110]* reflections of ZnO. The angle measured between the two legs in this perfect orientation, is 109°. The power spectrum of the nucleus is given in the inset at the left side of the nucleus, it exactely corresponds to the (110) face of the ZnO with the cubic structure of blende type, as described in [14, 15].

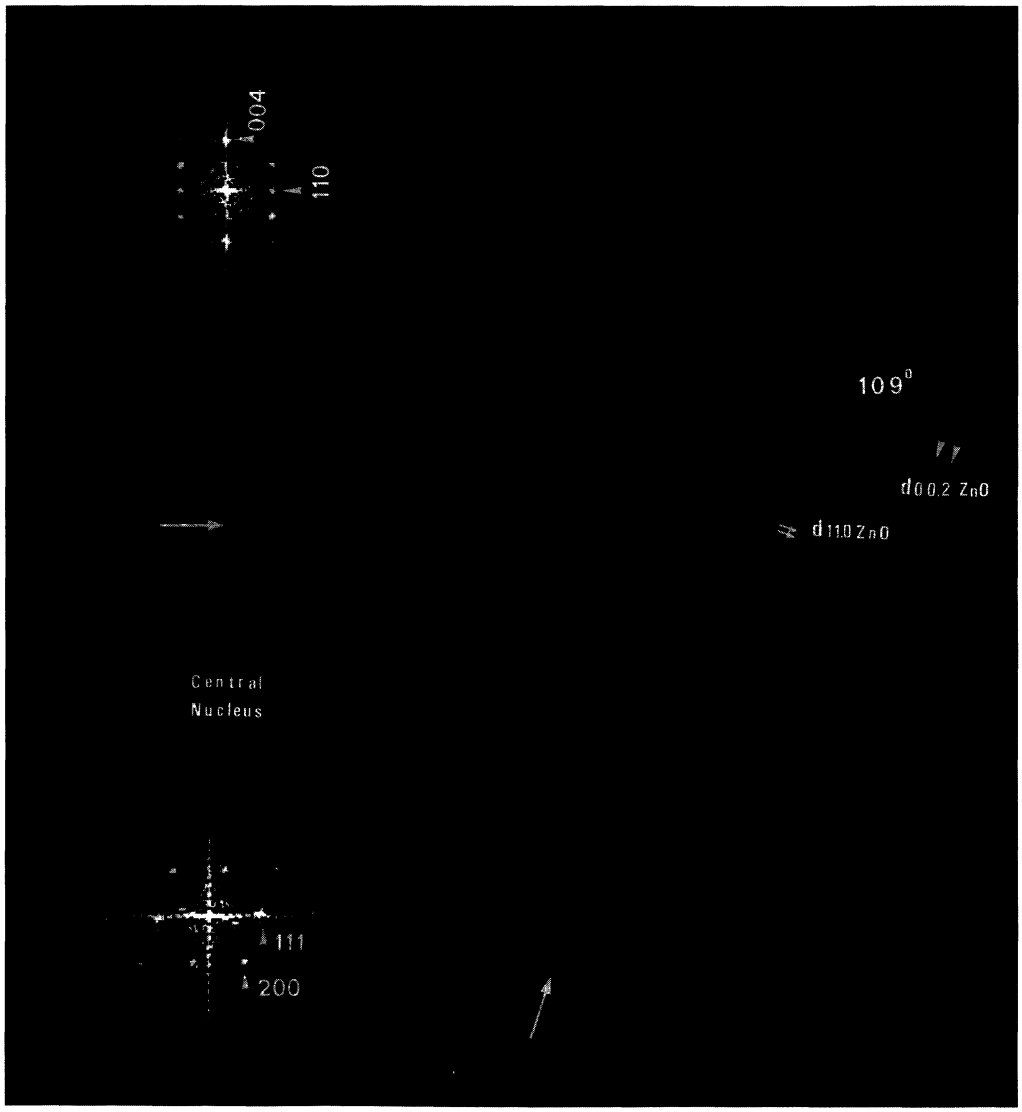

Fig. 2. — HRTEM image at 300 KV, of two ZnO legs in the same tetrapod, observed along their [210] directions. Power spectrum of the image of the leg in a [210] orientation (at the top) and Power spectrum of the image of the central nucleus (at the bottom).

Figure 3 shows a part of a ZnO prism [100] oriented where two lateral (1 $\bar{1}$.0) faces and the basal (00.1) faces are parallel to the electron beam. Compared to the long lateral faces, it is seen that the basal faces have a limited size and the lateral (10.0) faces are separared from the basal (00.1) faces by rounded parts. However, by using the preparation technique described above, polar (00.1) faces are more extended than in the commercial ZnO powder (Kadox 25, New Jersey Zinc Co.)) described in reference [18].

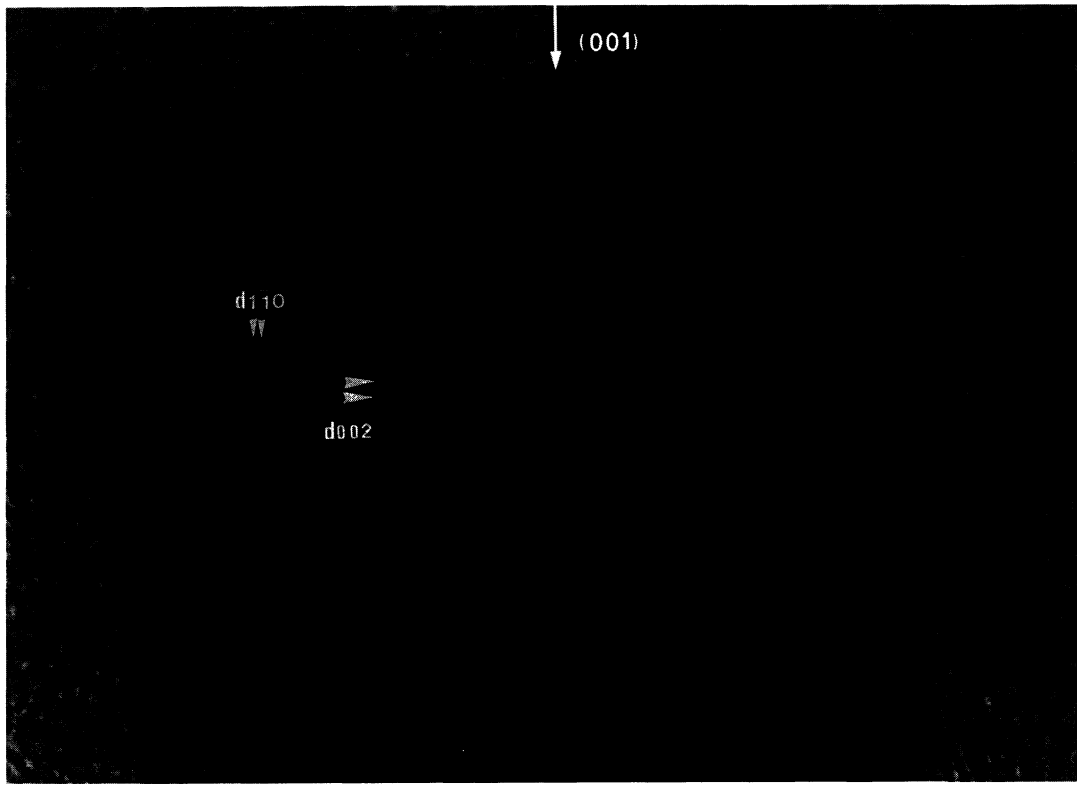

Fig. 3. — HRTEM image at 300 KV of the top of a ZnO prism [210] oriented, where two lateral (10.0) faces are normal to the electron beam and the basal (00.1) faces are parallel to the electron beam.

From HRTEM images of Pd particles grown on ZnO (10.0) faces seen in profile views [19], an epitaxial orientation between Pd and ZnO was found with the (211) Pd plane parallel to the (10.0) ZnO lateral face and the directions $[011]_{Pd} \parallel [001]_{ZnO}$. Figure 4 shows a Pd particle in profile view, on a lateral $(10\bar{1}0)$ face of ZnO. The interface plane between Pd and ZnO (10.0) is parallel to the electron beam so that the particle is seen along the [111] direction. This image was obtained with a Jeol 4000EX microscope in order to see the (220) lattice distances of small Pd particles with the distance of 0.137 nm.

The average ratio between the height and the basal diameter of the particles is approximately 0.4, which is the same as in the case of high temperature grown Pd on MgO (100) [1, 5].

When such a ZnO prism is oriented with two lateral faces (10.0) parallel to the electron beam (vertical), then, both other pairs of lateral faces make an angle of 30° with the horizontal plane.

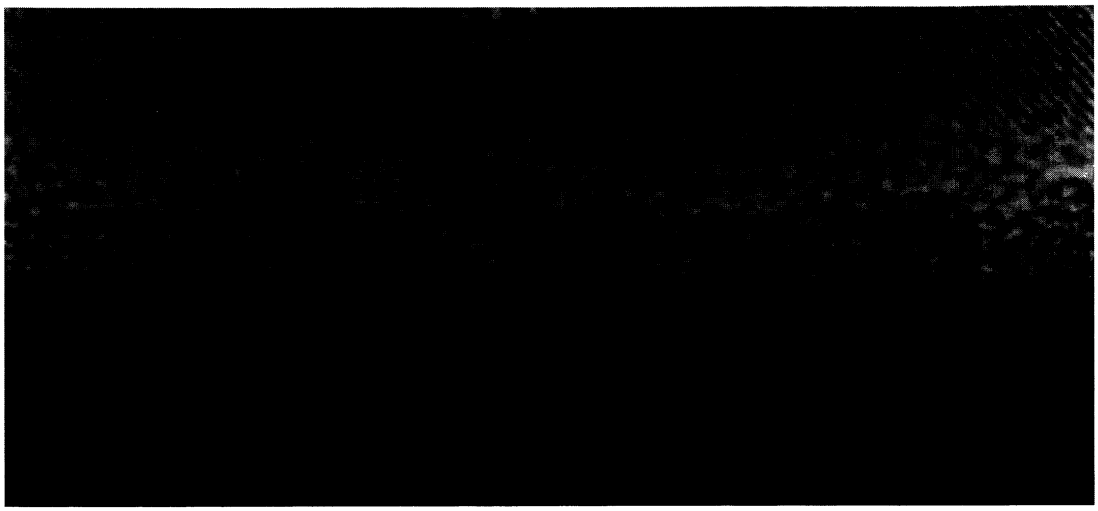

Fig. 4. — HRTEM image at 400 KV, of a prism [100] oriented with a pair of lateral faces parallel to the electron beam. In this orientation, particles are seen in profile view with the electron beam parallel to their interface with ZnO. They are seen along their [111] axis. The epitaxial relations are $(211)_{Pd} \parallel (10.0)_{ZnO}$ and $[011]_{Pd} \parallel [001]_{ZnO}$.

Therefore, the interface plane between Pd and ZnO $(1\ \bar{1}.0)$ or (01.0) are tilted by 30° compared to the horizontal plane.

On these faces $(1\ \bar{1}.0)$ and (01.0), Pd particles epitaxially oriented as described above, are imaged along the [110] axis or [100] axis tilted by 5° compared to the electron beam, and the ZnO is imaged with the (11.0) plane normal to the electron beam.

In Figure 5, the ZnO prism has two lateral sides (10.0) parallel to the electron beam, so the interface planes between Pd and ZnO (01.0) and $(1\ \bar{1}.0)$ are tilted by 30° compared to the horizontal plane. On the ZnO lattice, bright patches appear, most of them without distortions. The typical PS of a patch on ZnO (right inset) does not show any splitting or enlargement of the spots.

The contrast of these patches changes in the true focus series. They can be interpreted either as holes, large terraces in the ZnO, or as Pd particles.

The simulated diffraction pattern of Pd oriented on ZnO with the same relations as given before: [100]*Pd and [110]*ZnO parallel to the electron beam and $[01\ \bar{1}]_{Pd} \parallel [001]_{ZnO}$, is drawn in the left inset in Figure 5. The coincidence between spots from Pd and ZnO is nearly perfect even at long range order. In the PS of the experimental images, the main spots of Pd and ZnO are also superimposed. Indeed, the misfit between the lattices is 5% in the [001] direction of ZnO and 2% in the direction $[1\ \bar{1}0]$.

By tilting the ZnO prism by 15° around the [001] axis, from the orientation described in Figure 3, the lattice image of the ZnO desapears (except the 002 and 004 lattice fringes) but the particles are exactely seen along their [111] zone axis. Figure 6a shows such a prism with all the particles on the surface seen in the [111] orientation. This orientation with [220] Pd $\parallel [001]_{ZnO}$ is consistent with the epitaxial relationships: (211) Pd $\parallel (10.0)_{ZnO}$ lateral face and $[011]_{Pd} \parallel [001]_{ZnO}$.

The large particle in Figure 6b also corresponds to this orientation. All around the particle, in the thinnest parts, the contrast is modified. In this domain, the Pd lattice is dilated between 3 and 5% compared to the center of the particle. The splitting of the 220 spots in visible in the PS (see inset in Fig. 6b). It shows that the first deposited layers at the interface are deformed by the substrate.

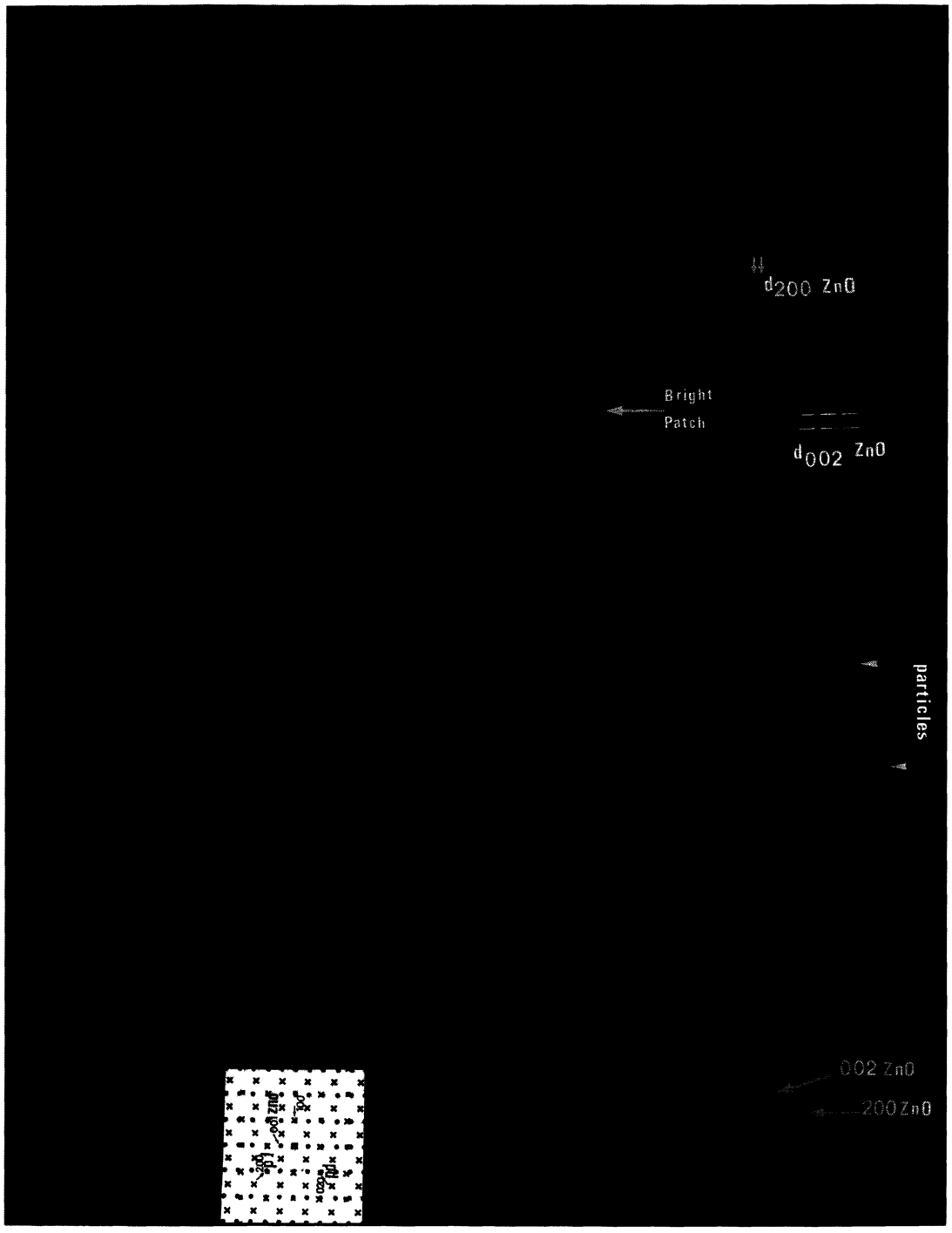

Fig. 5. — HRTEM image at 300 KV of a ZnO prism with two lateral (01.0) faces parallel to the electron beam, observed in a [100] direction, with bright patches on the faces and some flat particles in profile view. The PS of a bright patch on the ZnO lattice is shown in the right inset. The reciprocal lattices of Pd in the [100] zone axis, superimposed on ZnO with $(211)_{Pd} \parallel (10.0)_{ZnO}$ and $[01\,\bar{1}]_{Pd} \parallel [001]_{ZnO}$ is given in the left inset.

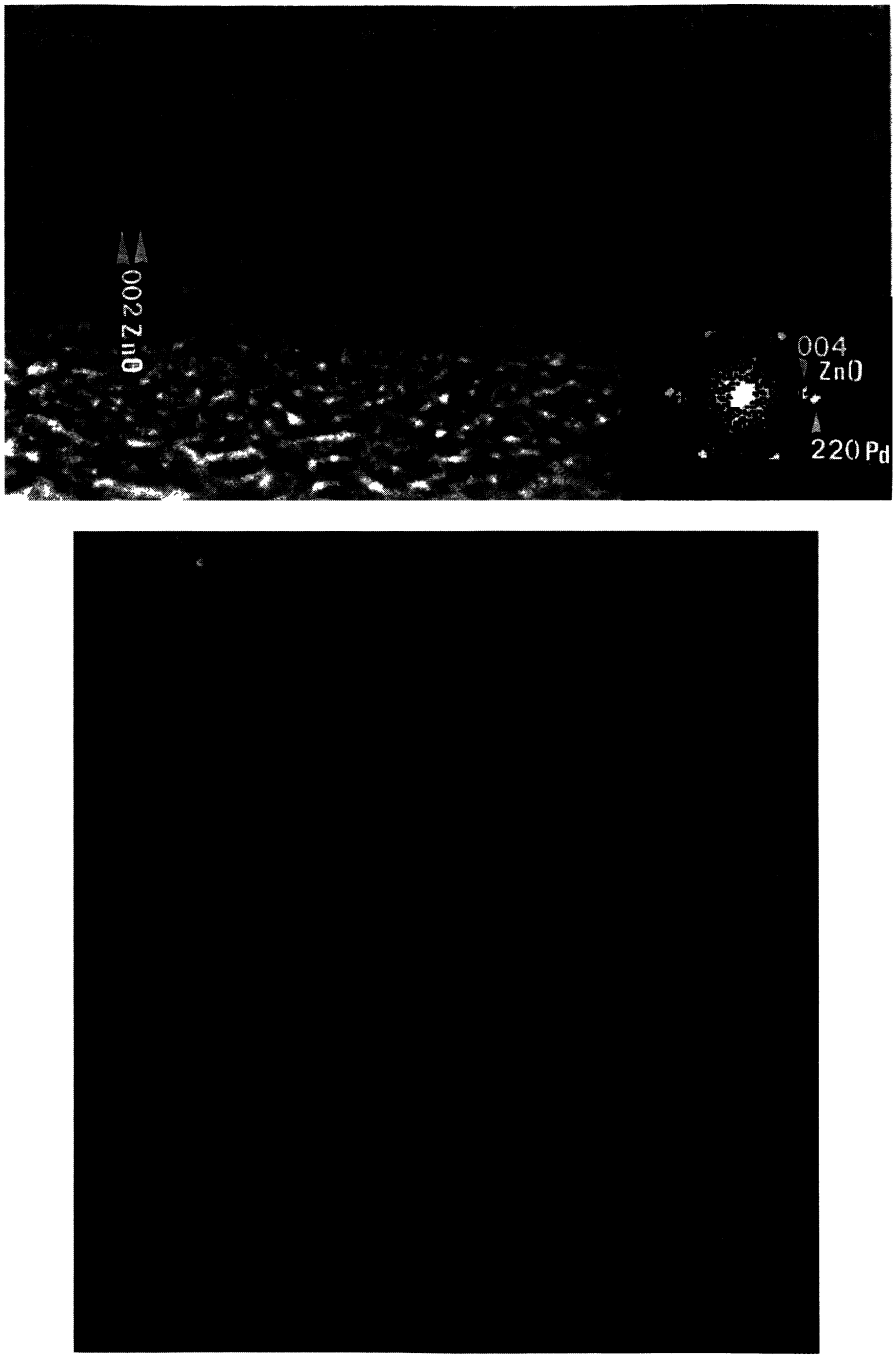

Fig. 6. — a) Small Pd particles (2 nm) in the (211) epitaxial orientation on ZnO. The ZnO prism is tilted by 15° around [001] compared to the image in Figure 3, so the particles are imaged in the [111] orientation. The power spectrum of the particles in the [111] zone axis is given in the inset. b) Large Pd particle (7 nm), seen in the [111] direction on ZnO. The Pd lattice is deformed at the interface. In the PS (inset) the spots are deformed.

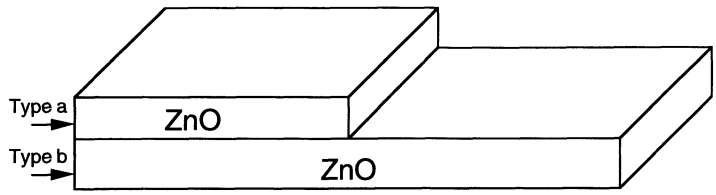

Fig. 7. — Schematic representation of the supercells of ZnO in the simulations of a terrace on a single layer of ZnO.

4. HRTEM Image Simulations

All the HRTEM images were simulated by the multislice method, using the EMS program written by Stadelman [20].

Holes at the surface of ZnO were simulated, for comparison with the bright patches without distortions, observed in the experimental images, as in Figure 6a.

The sampling was done with 256 × 256 pixels along the sides of a supercell (1.68 × 1.56 nm^2). A ZnO terrace, one ML thick, was simulated on the ZnO substrate. For this purpose, the first slice (type a) was cut into two parts, one full with ZnO, the other one empty. Then the next slices (type b) were filled with ZnO (see the drawing in Fig. 7). Figures 8a-i are obtained for a terrace (one slice type a) on one layer of ZnO (one slice of type b), here the edge of the terrace is clearly visible. For a terrace (one slice of type a) on a thick layer of ZnO (10 slices), the edge of the terrace is no longer visible, as seen in Figures 9.

To ascertain the origin of the bright patches, Pd layers on ZnO were also simulated in the same way. Five half layers of Pd were simulated on 20 full layers of ZnO. The sampling was done in 256 × 256 points for the size of the supercell: 2.81 × 2.75 nm^2.

The simulated images in Figure 10, show that Pd on ZnO in the epitaxial orientation described above, is represented as bright areas on the substrate, at a particular focus (70 nm).

The effect of the tilt of the sample on the HRTEM image is shown in Figures 11 and 12.

A thick ZnO crystal, (50 layers) is simulated with the perfect [100] orientation in the electron beam (Fig. 11a), then it is slightly tilted in the [001] direction in Fig. 12b), by 0.9°. The resolution is completely lost in the [001] direction. A very small particle, 1 nm in diameter is simulated in Figure 12a, then tilted by 5° in 12b. The intensity is slightly changed, but the resolution is not lost. Indeed, for such a small particle, the spots are enlarged in the reciprocal space, so that the image is not so sensitive to the orientation as for a large crystal. This explains that a better contrast is obtained from the supported particles than for the substrate, when the substrate is misoriented.

5. Discussion

Clean ZnO micro-crystals have been produced in situ by burning a Zn filament in a controlled atmosphere. Both single crystals and twinnned tetrapods were obtained, with the hexagonal structure. The HRTEM images of tetrapods perfectly oriented with two legs in the [100] zone axis give the evidence that the central nucleus limited by 8 (111) faces has the cubic structure of blende type, in agreement with several works [14, 15], instead of wurtzite type as previously claimed [16, 17].

Pd particles (1 – 7 nm) were grown at 450 °C in UHV on the lateral surfaces of the ZnO micro-crystals. The HRTEM images in top views of the particles are consistent with the images obtained

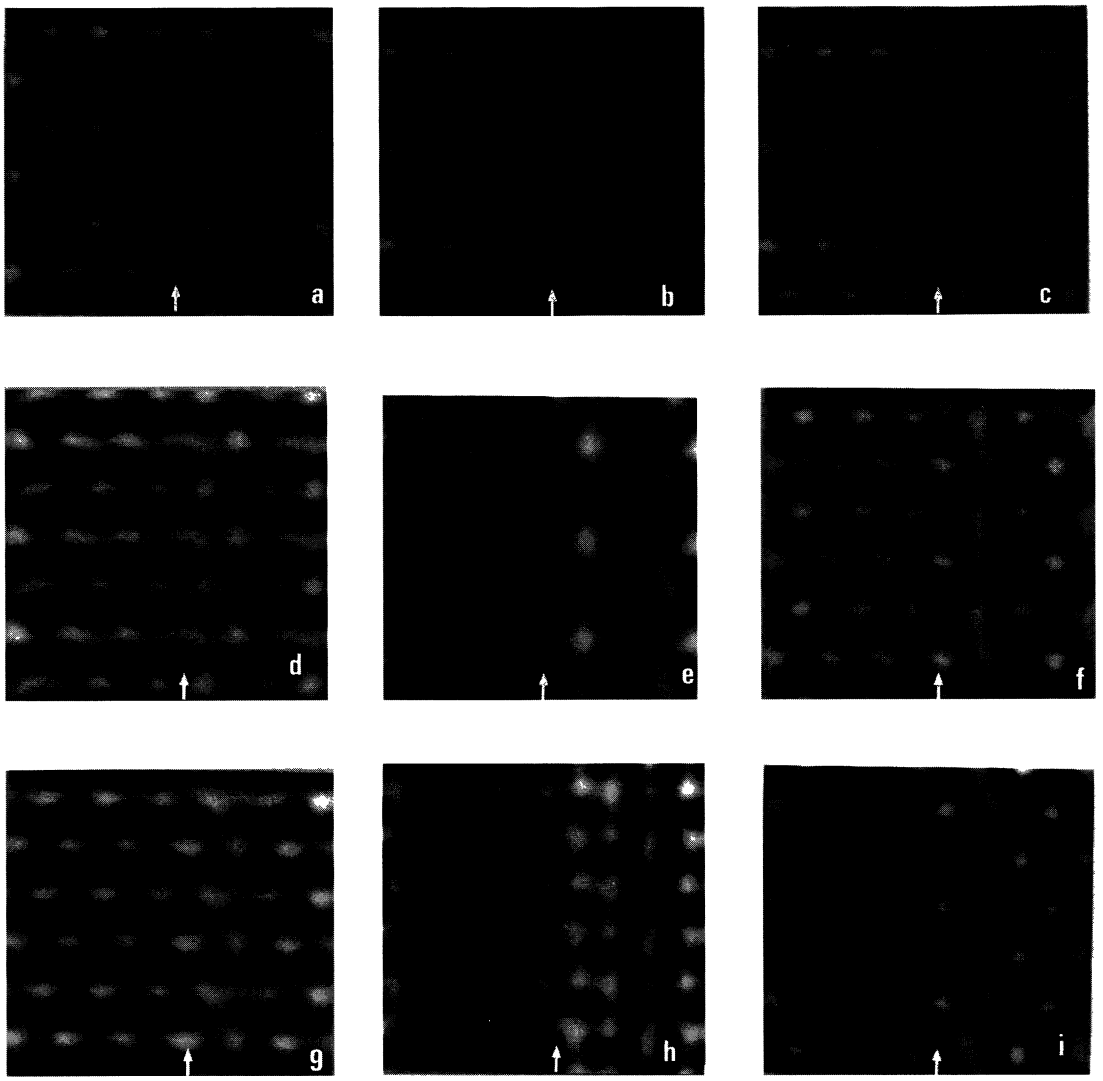

Fig. 8. — a-i) Simulated images of a terrace on one layer of ZnO (110), at the focus: −42, −52 (Scherzer focus), −62, −72, −82, −92, −102, −112 and −122 nm respectively. The hole is on the right side of all the images.

in profile view [19]. Most of the Pd particles are epitaxially oriented on ZnO with the relations: $(211)_{Pd} \parallel (10.0)_{ZnO}$ and $[011]_{Pd} \parallel [001]_{ZnO}$.

This orientation corresponds to small misfits between the lattices, 5% in the $[001]_{ZnO}$ and 2% in the $[110]_{ZnO}$ direction.

Pd particles have clearly a 3-dimensionnal shape. The growth mode of metals on ZnO single crystals is rather controversial. For Pd/ ZnO(00.1), layer by layer [21] or 3D clusters growth [11], are claimed.

For other metals like Cu, "pseudo" Stranski- Krastanov mode of growth [12, 13, 22] was found. However, it seems that 2D growth is a kinetic effect [13]. After annealing, only 3D clusters are

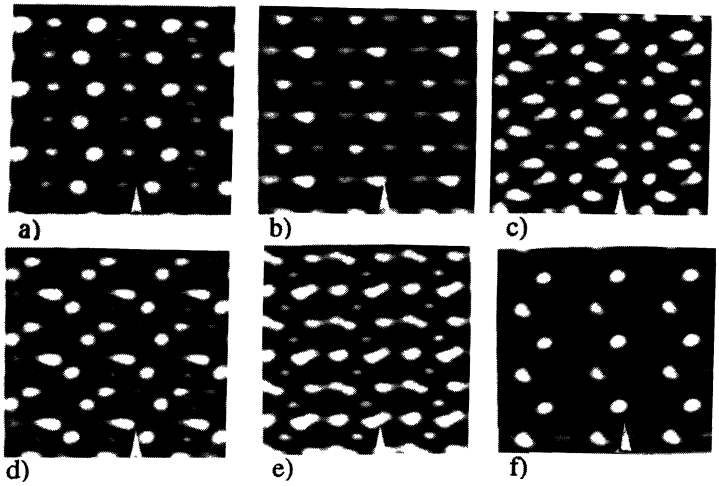

Fig. 9. — a-f) Simulated images of a terrace on a thick coating of ZnO (110), at the focus: −52 (Scherzer focus), −72, −82, −92, −102 and −112 nm respectively. The hole is at the right side of all the images.

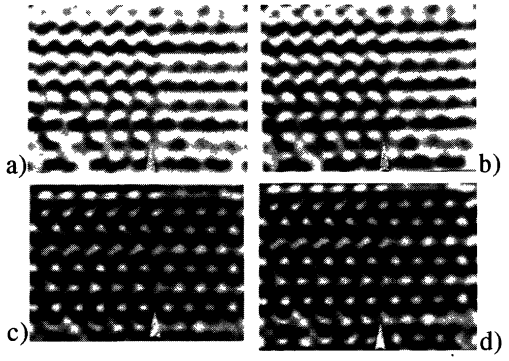

Fig. 10. — a-e) Simulated images of a Pd layer (211) oriented on ZnO (10.0), with $[011]_{Pd} \parallel [001]_{ZnO}$, seen along the [100] direction of ZnO and the [100] direction of Pd. The area with Pd is at the right side of the arrow. Focus: −52, −72, −92, −112 nm.

observed, indicating that the equilibrium growth mode is of Volmer Weber type. In our experiments, Pd is deposited at relatively high temperature (450 °C), then nearly equilibrium structure can be achieved by surface diffusion and 3D clusters are observed.

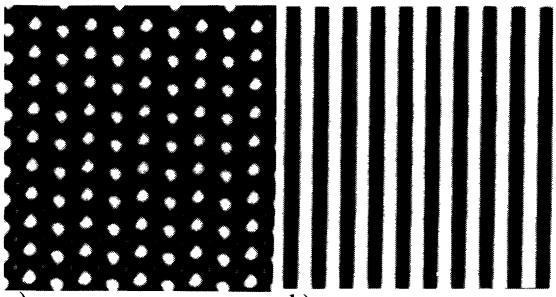

Fig. 11. — a, b) Simulated images of a ZnO crystal (50 layers thick) in the perfect [100] Bragg orientation a), and misoriented by 0.9° in the [001] direction b). a) and b) are imaged in the Scherzer conditions.

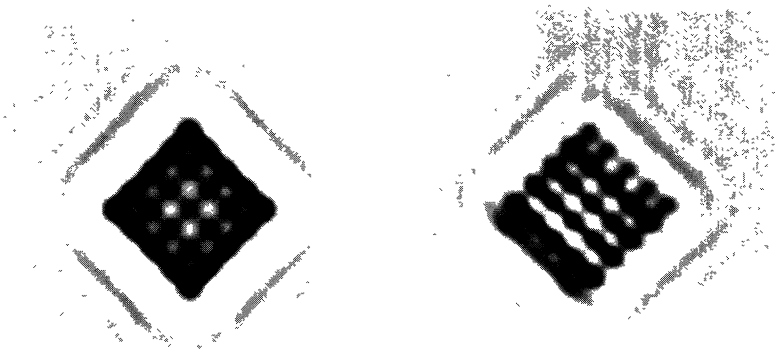

Fig. 12. — a, b) Small particle (1 nm) in the perfect (100) Bragg orientation a), and misoriented by 5° in the [001] direction b). a) and b) are imaged in the Scherzer conditions.

Acknowledgements

We thank C. Roucau from the LOE who gave us the opportunity to use the Philips CM 30 microscope and the CENG for the JEOL 4000 EX microscope.

References

[1] Henry C.R., Chapon C., Duriez C. and Giorgio S., *Surf. Sci.* **253** (1991) 177;
Duriez C., Henry C.R. and Chapon C., *Surf. Sci.* **253** (1991) 190.
[2] Jacobs J.M. and Schryvers D., *J. Catal.* **103** (1987) 436.
[3] Poppa H., Rumpf F., Moorhead R.D. and Henry C.R., *Mat. Res. Proc.* **3** (1988) 1.
[4] Yao M.H., Smith D.J. and Datye A.K., *Ultramicroscopy* **52** (1993) 282.
[5] Giorgio S., Henry C.R., Chapon C. and Penisson J.M., *J. Cryst. Growth* **100** (1990) 254.
[6] Fuchs G., Neiman D. and Poppa H., *Langmuir* **7** (1991) 2853.
[7] Ajayan P.M. and Marks L.D., *Nature* **338** (1989) 139.

[8] Ryndin Y.A., Hicks F., Bell A.T. and Yermakov Y.I., *J. Catal.* **70** (1981) 287.
[9] Klier K., *Appl. Surf. Sci.* **19** (1984) 267.
[10] Mokwa W., Kohl D. and Heiland G., *Z. Anal. Chem.* **314** (1983) 315.
[11] Jacobs H., Mokwa W., Kohl D. and Heiland G., *Surf. Sci.* **160** (1985) 217.
[12] Campbell C.T., Daube K.A. and White J.M., *Surf. Sci.* **182** (1987) 458.
[13] Campbell C.T. and Ludviksson K., *J. Vac. Sci. Technol.* **A12** (1994) 1825.
[14] Shiojiri M. and Kaito C., *J. Cryst. Growth* **52** (1981) 173.
[15] Kitano M., Hamabe T. and Maeda S., *J. Cryst. Growth* **128**(1993) 1099.
[16] Fujii M., Iwanaga H., Ichihara M. and Takeuchi S., *J. Cryst. Growth* **128** (1993) 1095.
[17] Iwanaga H., Fujii M. and Takeuchi S., *J. Cryst. Growth* **134** (1993) 275.
[18] Scarano D., Spoto G., Bordiga S., Zecchina A. and Lamberti C., *Surf. Sci.* **276** (1992) 281.
[19] Giorgio S., Henry C.R., Chapon C. and Nihoul G., Proceedings ICEM 13-Vol.2A, Applications in Mat. Sci., B. Jouffrey and C. Colliex Eds. (Les éditions de Physique, France, 1994) 349.
[20] Stadelmann P.A., *Ultramicroscopy* **21** (1987) 131.
[21] Gaebler W., Jacobi K. and Ranke W., *Surf. Sci.* **17** (1978) 355.
[22] Moller P.J. and Nerlov J., *Surf. Sci.* **307** (1994) 591.